PARTICULARITIES OF SINGLE SHEAR PIN JOINTS MODELING FOR MSC/NASTRAN

Adrian Viisoreanu, Ph.D.
Principal Engineer
Boeing Commercial Airplane Group
P.O. Box 7730, MS K09-52
Wichita Ks 67277-7730

Kris Wadolkowski
Technical Director
Aerostructures, Inc.
9666 Business Park Ave.
San Diego CA 92131

ABSTRACT

Inspired from the analysis of aircraft engine mount fittings, this paper presents techniques applicable to the solid modeling of single shear pin joints in MSC/NASTRAN. A parametric study describes the influence of some joint geometry parameters on the stress and bearing load distribution along the pin length. The effect of the residual stress induced by the bushing interference fit is also considered.

INTRODUCTION

Striving to produce faster, better, and cheaper aircraft, we often find the 'new frontier' as close as our own backyard, challenging well established but conservative assumptions.

A frequently used solution for the aircraft engine attachment to the strut is to have a single shear pin joint transfer the longitudinal and transversal loads, while tension bolts take the vertical forces. To meet the requirements for a quick engine change design, the number of these bolts is kept to a minimum, and on some models the engine thrust is reacted by a single shear pin.

The shear pin receptacle is usually located in a massive part of the engine mount fitting, that bears little resemblance with the typical lugs found in the stress manuals. When the exact distribution of the stress and bearing load is needed, the hand analysis methods are no longer satisfactory and we need to develop a detailed finite element model (FEM).

This paper presents some specific aspects of the shear pin modeling in MSC/NASTRAN, applicable to both single and double shear joints.

PROBLEM DEFINITION

The objective of this study was to accurately determine the stress concentration factor in the shear pin receptacle and the bearing load distribution along the length of the pin, using finite element modeling in MSC/PATRAN and finite element analysis with MSC/NASTRAN.

The linear distribution of the bearing load along the pin length assumed in some strength analyses is not very well suited for the fatigue and damage tolerance study, that demand a more precise stress value in the pin receptacle.

For a given shear load, the most important factor driving the stress in the shear pin receptacle is the joint geometry. Some parameters that influence the stress in the shear pin receptacle and the bearing load distribution along the pin length are **(Figure 1)**:

t/D	ratio between the plate thickness and the pin diameter
e	shear pin clearance
g	gap between the two plates
W/D	ratio between plate width and pin diameter
a/D	ratio between edge distance and pin diameter

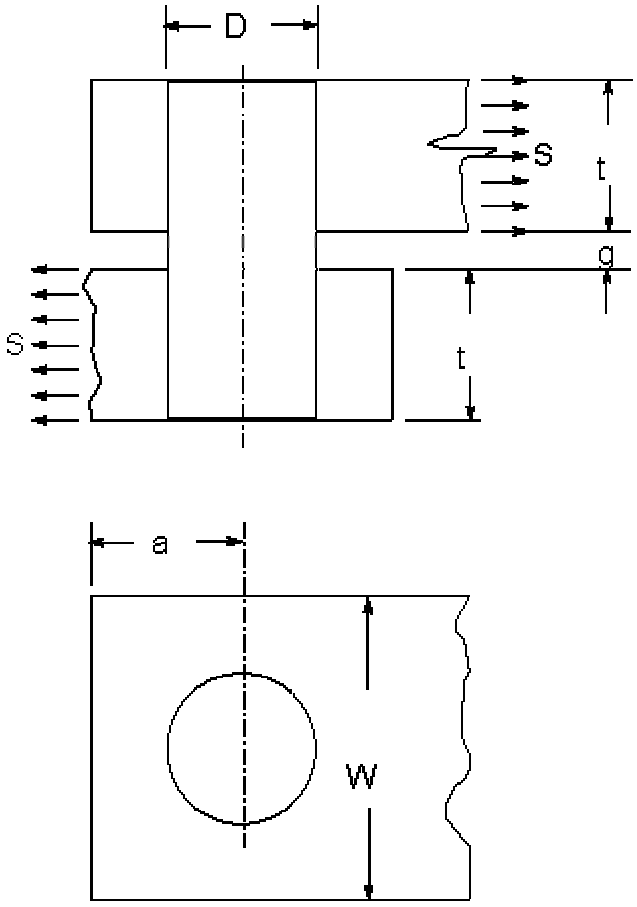

Figure 1. Single Shear Pin Joint Geometry

The residual stress caused by the shear pin bushing interference should also be added to the stress determined by the shear load. Usually small when compared with limit or ultimate stresses, the residual stress could have a significant influence on the fatigue and damage tolerance analysis.

Two generic solid finite element models were constructed in MSC/PATRAN to study the influence of these factors. The first finite element model was used to determine the residual stress caused by the shear pin bushing interference, while the other one was used to study the effect of the joint geometry on the stress concentration coefficient in the pin receptacle.

ANALYSIS

Bushing Interference Fit FEM

The bushing interference fit FEM contains a bushing and a fitting plate, connected

by adaptive gap elements (**Figure 2**). Since the gap loads are controlled by the displacement of the end nodes relative to the initial gap opening and not to the length of the gap element **[Reference 1 page 734]**, it is not required to make the bushing nodes coincident with those on the fitting.

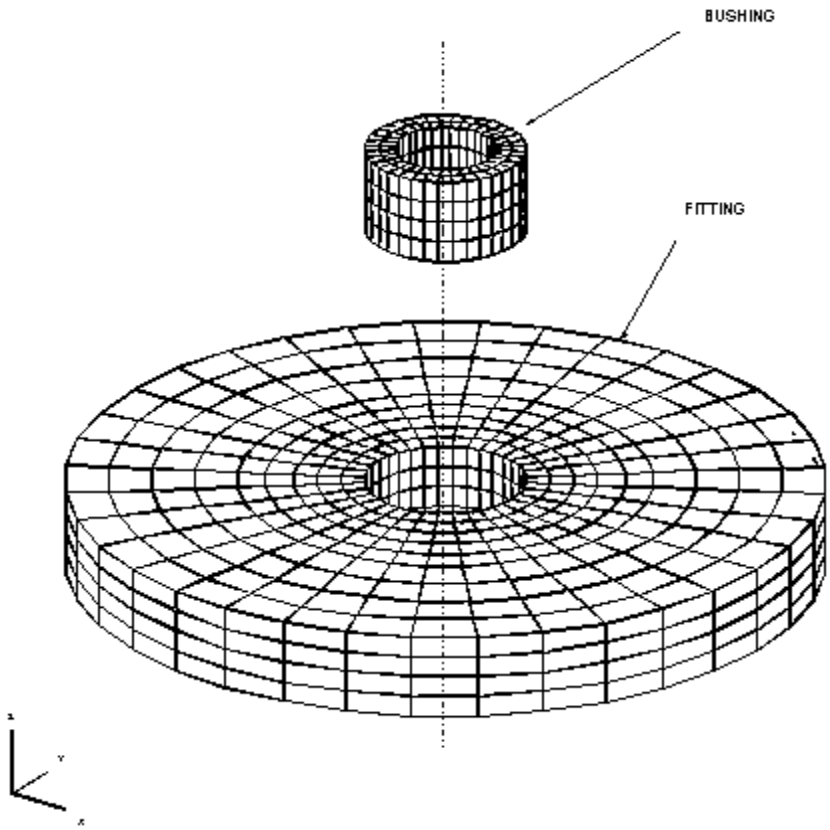

Figure 2. Bushing Interference Fit FEM
(bushing offset for clarity)

A 2-D model of the plate and bushing base was first constructed and meshed. Once a satisfactory mesh was obtained, the solid elements were constructed by extruding the 2-D mesh.

Gap elements were easily generated using MSC/PATRAN *Utilities/FEM Elements/ Create 1D Gap Elements.* All the GA nodes of the gap elements between the bushing and the fitting should be located on the bushing. A closed stiffness of 1.E+10 correctly modeled the behavior of the gap elements, while maintaining a reasonable convergence. Since the bushing presses onto the fitting, the initial gap opening was zero.

The gap properties were:

Gap Initial Opening: 0 IN
Closed Stiffness: 1.E+10 LB/IN
Sliding Stiffness: 100 LB/IN
Static Friction: 0.1
Kinematic Friction: 0.1
Max Penetration: 0.001 IN

Thermal expansion was used to model the bushing interference fit. Since element temperatures cannot be applied to solid elements, *NODAL* was selected in the MSC/PATRAN *Load/ Boundary Condition* form for temperature data input.

Two temperature load cases were defined. In the initial load case, both the bushing and the fitting nodes have the same temperature. For the final load case, the temperature of the bushing nodes was increased by:

$$\Delta t = \frac{D_{bushing} - D_{bore}}{\alpha D_{bore}} = \frac{e}{100\,\alpha}$$

where:

Δt	Temperature increase of bushing nodes (degrees)
$D_{bushing}$	Bushing outside diameter (in)
D_{bore}	Hole diameter (in)
e	Bushing interference (%)
α	Thermal expansion coefficient ($degree^{-1}$)

Although only the final subcase was needed, both subcases were selected in MSC/PATRAN / *Analysis / Subcase Select* to let the program write the temperature ID's for the initial state. The MSC/NASTRAN input deck generated by MSC/PATRAN was modified in order for MSC/NASTRAN to run correctly.

In the following example the commented cards were removed from the MSC/PATRAN generated bulk data file, while the one in bold italics was manually inserted. The temperature load ID for the initial subcase was 2, while 1 corresponds to the final temperature.

```
$ TEMPERATURE(MATERIAL) = 1
TEMPERATURE (INITIAL) = 2
SUBCASE 1
$ Subcase name : final
SUBTITLE=final
NLPARM = 1
SPC = 2
TEMPERATURE(LOAD) = 1
DISPLACEMENT(PLOT,SORT1,REAL)=ALL
SPCFORCES(PLOT,SORT1,REAL)=ALL
STRESS(PLOT,SORT1,REAL,VONMISES,BILIN)=ALL
$
$ SUBCASE 2
$ Subcase name : initial
$ SUBTITLE=initial
$ NLPARM = 2
$ SPC = 2
```

```
$ TEMPERATURE(LOAD) = 2
$ DISPLACEMENT(PLOT,SORT1,REAL)=ALL
$ SPCFORCES(PLOT,SORT1,REAL)=ALL
$ STRESS(PLOT,SORT1,REAL,VONMISES,BILIN)=ALL
```

To avoid the thermal expansion of the bushing along its axis, the bushing material was defined as 3d orthotropic with $E_1 = E_2 = E_3 = E_{isotropic}$, $G_1 = G_2 = G_3 = G_{isotropic}$, and Poisson's coefficients coupled with the axis direction null ($\nu_{13} = \nu_{23} = 0$).

Shear Pin FEM

The shear pin FEM contains two plates and a shear pin. The shear load (*S*) was applied as uniformly distributed pressure on the frontal face of the lower plate, while the upper plate was constrained at the other end (**Figure 3**).

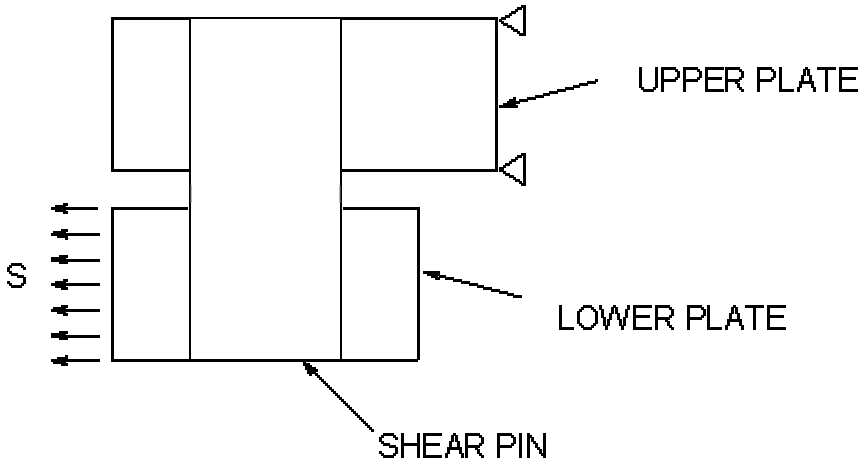

Figure 3. Shear Pin FEM Boundary Conditions

To take advantage of symmetry, only half of the joint was modeled. Starting from an initial model, several others were generated by changing different joint parameters (**Figure 4**).

The shear pin is connected to the two plates by adaptive gap elements. The properties of the gap elements were same as in the bushing model, with the exception of the initial gap opening that corresponds to the actual clearance between the shear pin and its receptacle.

Since all gap elements were opened in the initial phase, the stiffness of the joint was quite small. To avoid convergence problems, the load applied in the first step should not cause excessive displacements. For this model the first subcase shear load was 1000 lbs., achieved in 20 increments of 50 lbs. each.

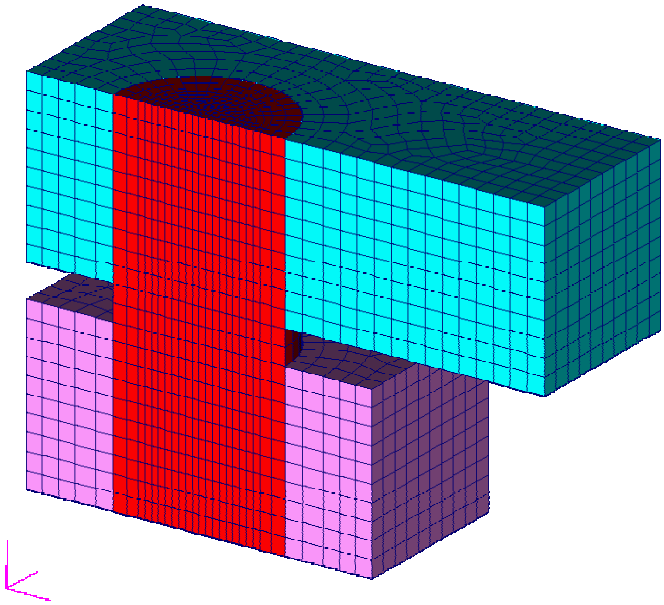

Figure 4. Shear Pin Joint FEM

DISCUSSION

The MSC/NASTRAN non-linear solution was used for this analysis (solution 106). Since the relative displacements in the shear pin joint are small, the large deformations option was turned off in MSC/PATRAN */ Analysis / Solution Type / Solution Parameters.*

Because the gap elements do not have a differential stiffness matrix, their behavior is not affected by the large displacement option **[Reference 2, page 750]**. For comparison, one test run was performed with the large displacement option on. The maximum stress change was only 1.08 %, while the execution time increased by 96%.

The bushing interference model was used to determine the residual stress. For a steel bushing in a titanium plate with an interference of 0.126%, the residual stress was 9.291 Ksi, about 4% higher than an alternative hand analysis method indicated (**Figure 5**). The residual stress decreased as we moved away from the hole, and

leveled off when the distance from the hole center was greater that twice the diameter (**Figure 6**).

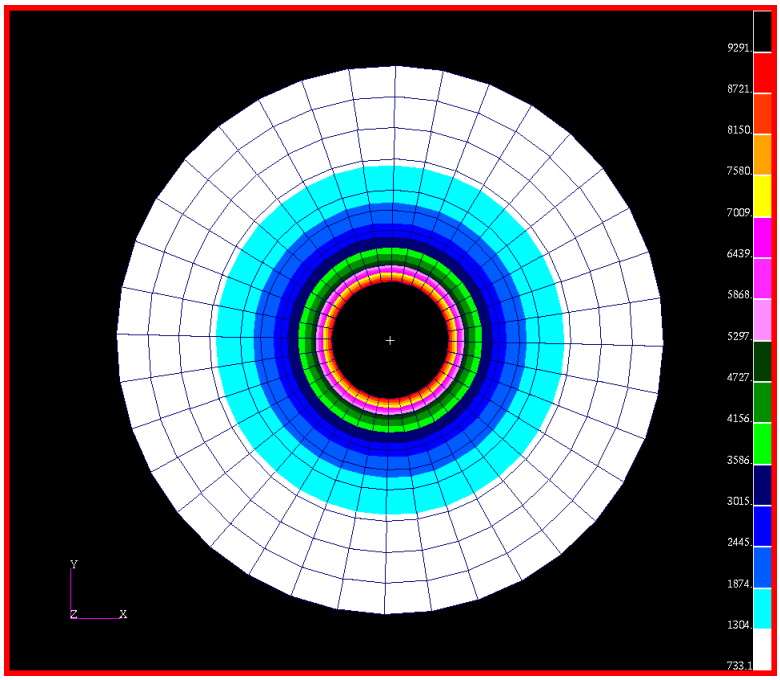

Figure 5. Bushing Interference Stress

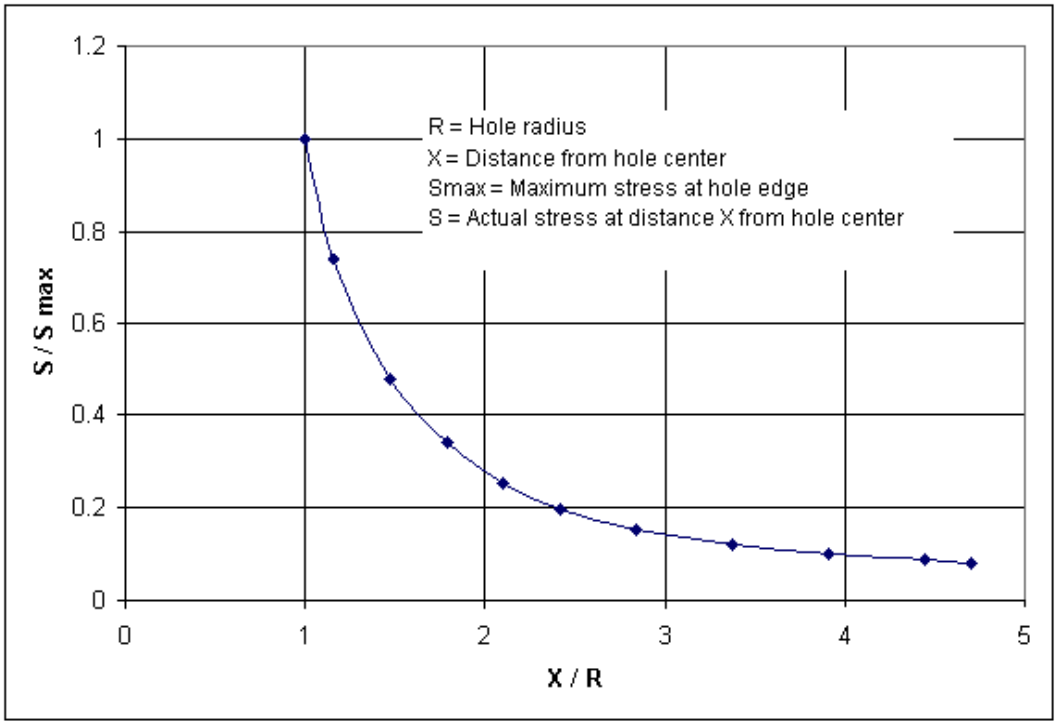

Figure 6. Residual Stress vs. Distance from Hole Center

Although small compared with the limit or ultimate stress, the residual stress determines a notable change in the fatigue and damage tolerance results. For an example spectrum, a 2 Ksi farfield residual stress determined a 10% increase in the stress factor, significantly affecting the crack growth rates (**Table 1**).

Residual Stress (Ksi)	0	2
Stress Factor (Ksi)	16	17.6
Fatigue Margin	1.34	1.22
Max. Fatigue Stress (Ksi)	10.45	12.45

Table 1. Effect of Bushing Residual Stress on Fatigue and Crack Growth Parameters

The shear pin model was modified to study the effect of different parameters on the stress concentration factor and on the bearing load distribution along the shear pin. The maximum stress in the receptacle was found close to the inner face of the plates (**Figure 7**).

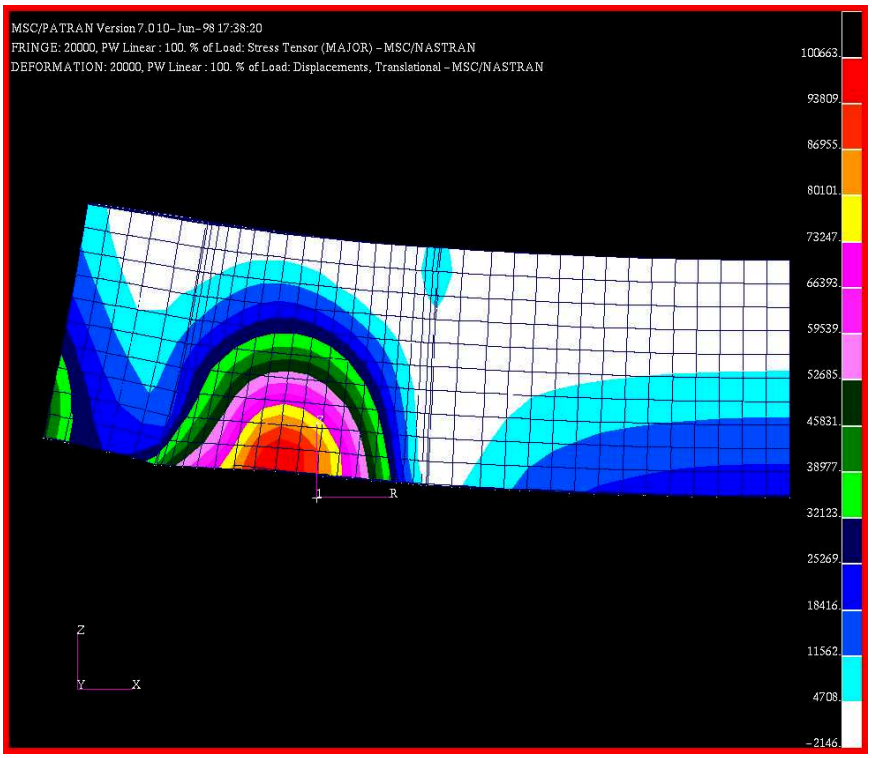

Figure 7. Stress and Deformation of Shear Pin Upper Receptacle

Most of the bearing load was taken by the elements close to the plate faces, while the middle ones were practically not loaded. When the plates were supported along three edges rather than one, the bearing load decreased and its distribution along the pin axis changed (**Figure 8**).

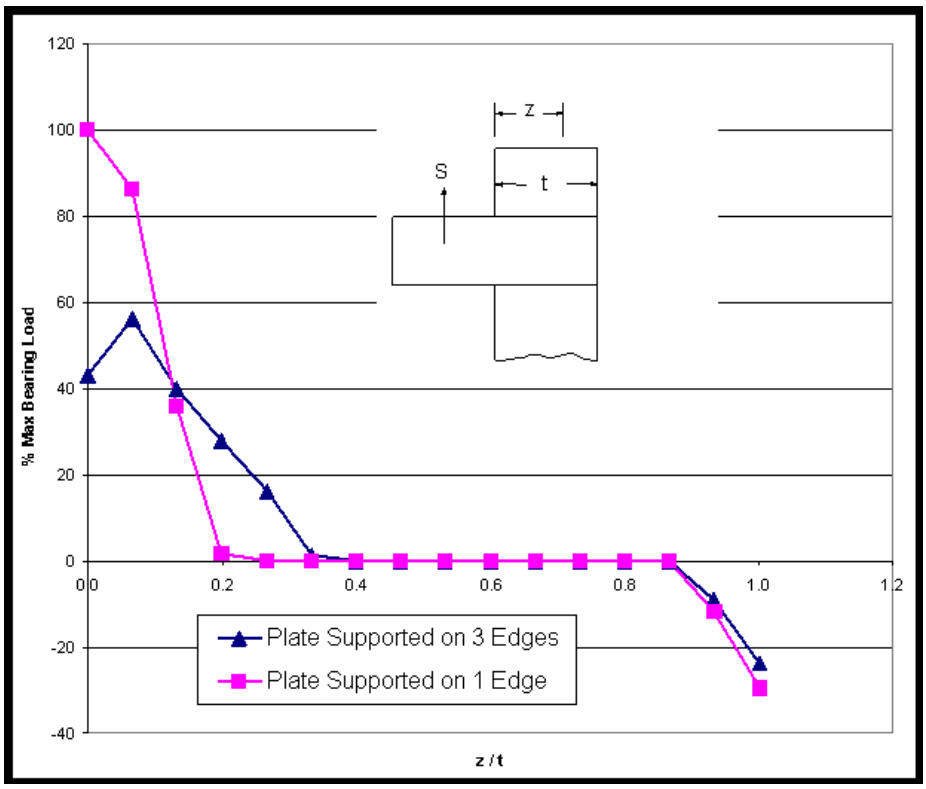

Figure 8. Bearing Load Distribution along Shear Pin Axis

As the thickness of the plate increased, so did the bending moment created by the shear load. Since most of the load transfer took place near the edge of the receptacle while the middle elements were ineffective, the enlargement of the plate thickness resulted in an increase of the stress concentration coefficient (**Figure 9**).

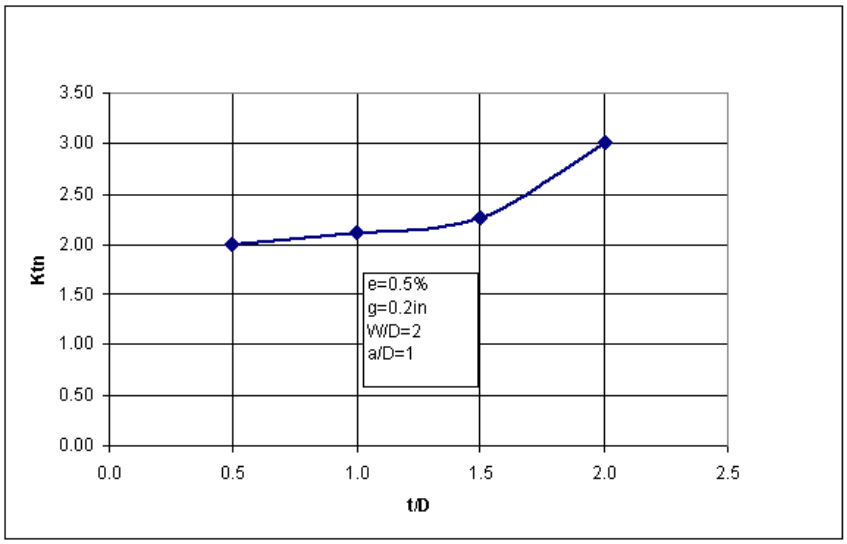

Figure 9. Effect of Plate Thickness

CONCLUSIONS

This paper showed some modeling techniques that can be applied to the construction of other shear pin joint FEM's. Data presented in this paper is intended to show the influence some of the joint parameters have on the stress and bearing load distribution along the pin axis.

The stress and bearing load distribution along the shear pin receptacle are dependent on the joint geometry and on the boundary conditions. Plots could be generated for each of the joint parameters and used to calculate the stress concentration without having to build a FEM for each individual geometry.

The influence of the residual stress induced by the bushing interference fit is small compared to the usual limit or ultimate loads, but can have a significant detrimental effect on the fatigue and damage tolerance behavior of the structure.

The stress and bearing load distribution is non-linear, with the elements close to the

plate faces transferring most of the load. Compared with the assumption that the bearing load varies linearly along the shear pin length, the finite element analysis resulted in a lower pin bending, but a higher bearing stress.

Some features of MSC/PATRAN proved especially helpful and shortened the time required to construct the models used in this study. The capability to generate solid elements by extruding a 2-D mesh works very well for paralelepipedic and cylindrical bodies.

The '*Create Gap Elements*' utility was essential in generating the gap elements between the pin, bushing, and fitting plate. This action was achieved very easy with a few mouse clicks.

The MSC/NASTRAN v.70 '*Adaptive Gap Element*' was a useful feature for this model, allowing the program to adjust the stiffness of the gap elements in order to avoid excessive penetration of the parts in contact. Setting a high initial gap stiffness to avert the element penetration created convergence problems in earlier versions of MSC/NASTRAN.

ACKNOWLEDGEMENTS

The author would like to thank:

Dr. Alexander Rutman for his pointed critique of some hand analysis assumptions that provided the original motivation of this study.

Gary Cassatt who encouraged me to attend the conference.

Anna Howart who helped me get all the forms ready just in time to meet impossible deadlines.

Rita Prettyman and Dan Stadler from MSC, for their effort in organizing this conference.

REFERENCES

1. *MSC/NASTRAN Version 70 Quick Reference Guide*, The MacNeal-Schwendler Corporation, Los Angeles, CA 1997

2. *MSC/NASTRAN Version 68 Reference Manual,* The MacNeal-Schwendler Corporation, Los Angeles, CA 1995